Quantifying total suspended sediment export from the Burdekin River catchment using the loads regression estimator tool

Petra M. Kuhnert,[1] Brent L. Henderson,[2] Stephen E. Lewis,[3] Zoe T. Bainbridge,[3] Scott N. Wilkinson,[4] and Jon E. Brodie[3]

[1]   The loads regression estimator (LRE) was introduced by Wang et al. (2011) as an improved approach for quantifying the export of loads and the corresponding uncertainty from river systems, where data are limited. We extend this methodology and show how LRE can be used to analyze a 24 year record of total suspended sediment concentrations for the Burdekin River. For large catchments with highly variable discharge such as that of the Burdekin River, it is important to quantify loads and their uncertainties accurately to determine the current load and to monitor the effect of changes in catchment management. The extended methodology incorporates (1) multiple discounted flow terms to represent the effect of flow history on concentration, (2) a term that captures sediment trapping and spatial sources of flow in terms of the ratio of flow from above the Burdekin Falls Dam, and (3) catchment vegetation cover. Furthermore, we validated model structure and performance in relation to the application tested. We also considered errors in gauged flow rates of 10% that were consistent with the literature. The results for the Burdekin site indicate substantial variability in loads across years. The inclusion of vegetation cover as a predictor had a significant impact on total suspended sediment (TSS) concentration, with values up to 2.1% lower noted per increasing percentage of vegetation cover. TSS concentration was up to 38% lower in years with greater proportions of flow from above the dam. The extended LRE methodology resulted in improved model performance. The results suggest that management of vegetation cover in dry years can reduce TSS loads from the Burdekin catchment, and this is the focus of future work.

1.   Introduction

[2]   Sediments and nutrients are high-priority river contaminants that can significantly affect freshwater and receiving estuarine and marine environments [*Brodie et al.*, 2012; *De'ath and Fabricius*, 2010; *Doney*, 2010; *Furnas*, 2003]. In the Great Barrier Reef (GBR) catchment area in northeastern Australia, a strong emphasis is placed on quantifying pollutant loads (suspended sediments, nutrients and pesticides) and their sources of uncertainty for the purpose of detecting trends in loads [*Reef Water Quality Protection Plan Secretariat*, 2009]. Estimates of loads with associated uncertainty from monitoring data are therefore required to determine current baseline exports, sources of

pollution and a means to assess progress toward Australian and Queensland government "reef plan" targets. Although this could be met by improvements to measurement programs that focus on frequent sampling, in reality monitoring records will often contain gaps because of equipment failure or impaired site access. Even where sampling is reliable and representative, in variable climates it is desirable to utilize the available historical monitoring records of variable sampling frequency for assessing long-term loads. For monitoring current and future total suspended sediment (TSS) loads, turbidity meters can provide an alternative to statistical analysis of measured TSS concentrations, particularly in smaller channels where TSS concentrations can be highly variable during runoff events. However, the cost of deploying and maintaining these instruments means that standard TSS monitoring continues to be used at many sites. Furthermore, turbidity meters must be calibrated against measured TSS concentrations in water samples from the site. At large river cross sections variation with depth in the suspended concentration of sand can be an additional complication. For example, a transmissometer, described in the paper by *Mitchell and Furnas* [2001] was tested in the GBR catchment area. Because of the extreme depth range of the Burdekin River between low flow

[1]CSIRO Mathematics, Informatics and Statistics, Glen Osmond, South Australia, Australia.
[2]CSIRO Mathematics, Informatics and Statistics, Canberra, ACT, Australia.
[3]Centre for Tropical Water and Aquatic Ecosystem Research (TropWATER), Australian Tropical Sciences Innovation Precinct (ATSIP), James Cook University, Townsville, Queensland, Australia.
[4]CSIRO Land and Water, Canberra, ACT, Australia.

(where depth was minimal) and high flow (tens of meters), the probe was positioned near the bottom. However, a robust relationship between a transmissometer reading of turbidity and TSS in mg L^{-1} could not be developed. For several reasons therefore, a predictive load estimation tool incorporating explanatory variables and providing some diagnostic capability is useful for analyzing TSS concentrations and loads in large, complex and highly variable river systems.

[3] Estimating pollutant loads at river stations typically requires models that predict temporal patterns of pollutant concentration between sampling times [*Asselman*, 2000]. To date, methods used to calculate pollutant loads in the GBR consist of the popular ratio estimators and linear interpolation [*Cooper and Watts*, 2002; *Letcher et al.*, 2002; *Littlewood and Marsh*, 2005]. However, these estimators lack flexibility as they cannot identify the major contributors and sources of contaminants. They also do not provide estimates of uncertainty in concentration and flow rates and therefore do not incorporate those into standard error calculations, if indeed they are provided. Furthermore, they cannot quantify the loads in years where pollutant concentrations are poorly sampled or missing.

[4] Rating curves have been a widely used method for estimating pollutant loads and quantifying the respective uncertainty [*Cohn*, 1995; *Cohn et al.*, 1992; *Rustomji and Wilkinson*, 2008; *Thomas*, 1985, 1988; *Thomas and Lewis*, 1995; *Walling*, 1977; *Wang et al.*, 2011]. The latest of these approaches by *Wang et al.* [2011] provides estimates of loads from monitoring data and has recently been used to provide baseline estimates of loads for reporting [*Kroon et al.*, 2012] as well as provide a framework for sample size estimation to determine the number of years of monitoring data required to detect trends [*Darnell et al.*, 2012]. The method proposed by *Wang et al.* [2011], which we refer to as the Loads Regression Estimator, hereafter termed LRE, is based upon the traditional rating curve approach by *Cohn et al.* [1992] but extends the methodology to incorporate hydrological variables that attempt to mimic temporal characteristics of a river system using a flexible generalized additive modeling (GAM) framework. The method incorporates key measures of uncertainty: measurement error in the sampled flow and concentration; model uncertainty arising from a lack of understanding of the underlying hydrological processes; and sampling uncertainty arising from the way in which flow and concentration are sampled, i.e., more frequently during high-intensity discharge events. In addition to accommodating uncertainties in concentration, errors in flow rates can be directly incorporated into the uncertainty calculation of the loads estimate. Furthermore, this framework develops a historical representation of concentration and flow for the system, enabling the estimation of loads for years where no monitoring data were collected. Of course, the accuracy of the loads in these instances is subject to how well the model captures the system processes.

[5] In this paper we extend the LRE methodology proposed by *Wang et al.* [2011] to cater for highly variable river systems where monitoring data are limited. The LRE methodology and its extensions are illustrated using a long-term record of total suspended sediment sampled at the Inkerman Bridge site on the Burdekin River. As the Burdekin catchment represents one of the driest and largest catchments in the GBR catchment area, data captured at the Inkerman Bridge site are limited through the period 1986–2010. The primary purpose of the LRE applied to this site is to derive best estimates of past sediment yield to establish a baseline for assessing future changes.

2. Case Study: Inkerman Bridge, Burdekin River

2.1. Catchment Characteristics

[6] The Burdekin River drains the second largest basin (area $\sim$130,000 km^2) draining to the GBR lagoon and it represents the largest in terms of mean gauged annual discharge and total annual sediment export to the GBR [*Furnas*, 2003] (Figure 1). Cattle grazing represents the dominant land use within the catchment (95%) with the remaining 5% composed of other uses, including cropping [*Furnas*, 2003]. The geology of the catchment is quite varied containing igneous, sedimentary and metamorphic rock provinces [*Bainbridge et al.*, 2008] and a wide variety of soil types. Precipitation within the catchment occurs primarily within a well-defined, summer wet season with higher falls near the coast and in the northern parts of the catchment [*Amos et al.*, 2004; *Furnas*, 2003]. The annual discharge of northern Australian rivers is highly variable in Australian and world terms [*Petheram et al.*, 2008]. The recorded annual discharge of the Burdekin River at Inkerman Bridge (water year: October 1 to September 30) ranges from 247,110 ML (1930/1931) to 54,066,311 ML (1973/1974) over the 90 year record to 2010. Development of the catchment by European settlers began in the mid-1800s with the introduction of sheep and cattle [*Lewis et al.*, 2007] and the commencement of alluvial mining. It is generally accepted these activities would have increased the annual average flux of sediment to the GBR lagoon [*Belperio*, 1979; *McKergow et al.*, 2005] and trace element analysis of coral cores has provided evidence in support of that proposition [*Lewis et al.*, 2007; *McCulloch et al.*, 2003].

[7] Several attempts have been made to estimate the current "annual average" suspended sediment export and the "natural" (pre-European settlement) load for the Burdekin River. The first estimate was reported by *Belperio* [1979], who used a regression-based sediment rating curve approach to calculate an annual average load of 3.45 $\times$ 10^6 t using monitoring data from the 1970s. Since then annual average suspended sediment load estimates (summarized by *Brodie et al.* [2009, Table 5]) have been derived using monitoring data (estimates range between 3.8 and 4.6 $\times$10^6 t) and catchment models (2.4–9.0 $\times$10^6 t yr^{-1}) with some models also predicting 'natural' loads (0.48–2.1 $\times$ 10^6 t). We note that no previous load calculations have included an estimate of the uncertainty apart from the recent work by *Kroon et al.* [2012] that used a base LRE model to obtain average annual estimates of loads.

2.2. TSS Sampling at Inkerman Bridge on the Burdekin River

[8] TSS data were collected from the Inkerman Bridge site on the Burdekin River between 1986 and 2010 (692 samples spanning 24 water years). This site is 20 river km upstream of the river mouth, with a catchment area of
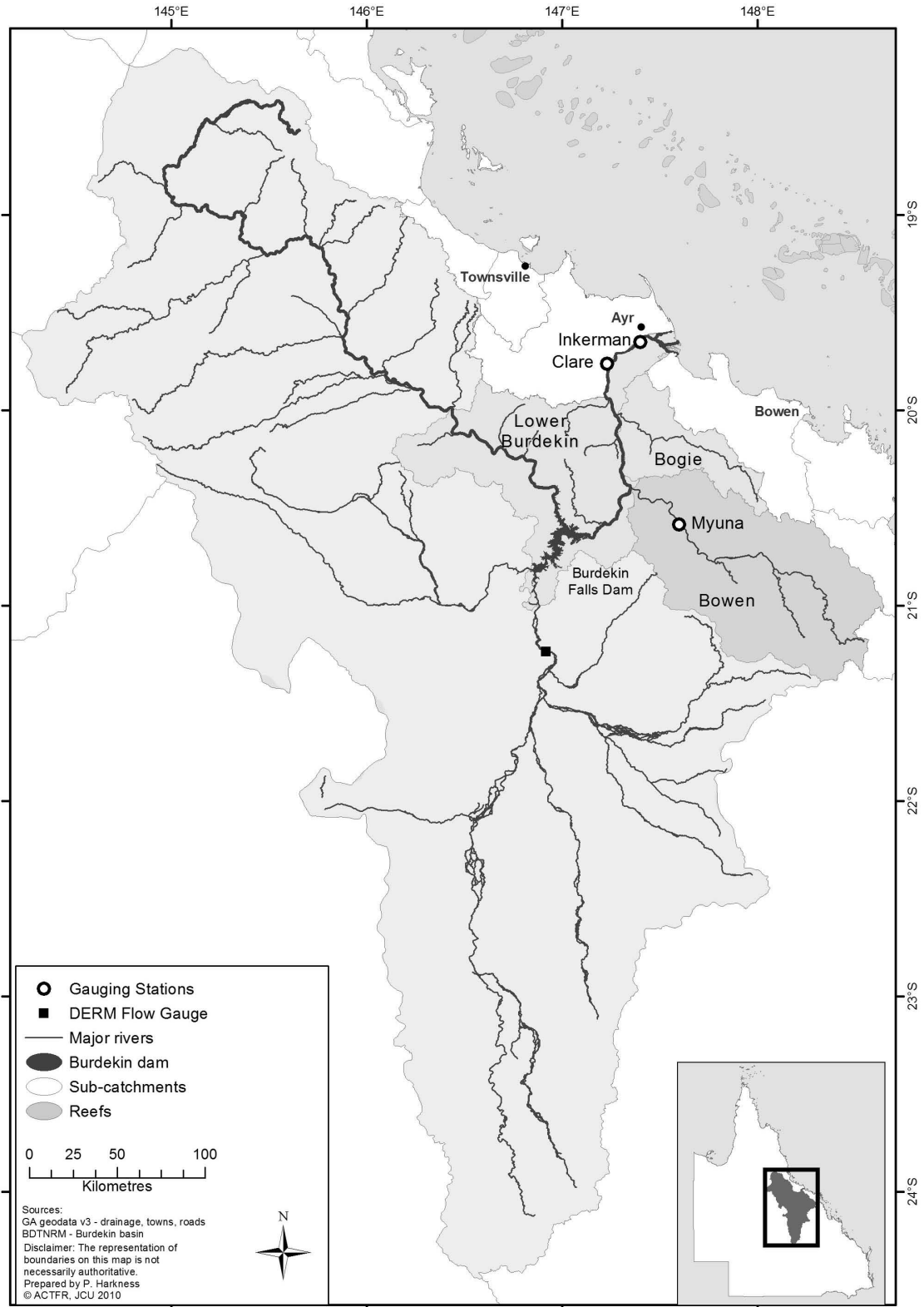
Figure 1. Map of the Burdekin catchment showing the Inkerman Bridge sampling site where total suspended sediment (TSS) samples were taken for this study. Flow samples were collected at the Inkerman gauge at Ayr.

~130,000 km². TSS samples were collected from the sur-face of the river (top 50 cm of water column). Samples were collected from the center of the channel flow over the rising, peak and falling stages of the flow hydrograph as well as during base flow conditions. Particle size analysis of the routine surface TSS samples as used in this study show that they are predominantly silt and clay size fractions, with a small amount of sand which is generally less than 10% of total mass [*Bainbridge et al.*, 2012]. Measurements of sus-pended sediment across the cross section and through the depth profile of the Burdekin River in the vicinity of Inker-man also found that sand composes less than 10% of the TSS concentration at the surface [*Belperio*, 1979, Figures 5 and 6; *Amos et al.*, 2004, Figure 8]. Further, these two latter studies show that the surface concentrations of silt and clay in the Burdekin River are representative of the entire cross section, and thus the load estimates in the present study are considered representative of the combined silt-clay size fractions. While the concentration of sand transported in suspension does increase with depth below the water sur-face [*Belperio*, 1979], sand load is not of interest for assess-ing TSS impacts beyond its point of deposition near the river mouth.

[9] The samples were cooled and transported to the labo-ratory for analysis. The samples have been collected through a number of programs and research providers over the 24 year period by the Australian Institute of Marine Sci-ence, the Queensland Department of Environment and Resource Management (DERM: both surface water data archive and GBR Loads Monitoring programs), University of Queensland and North Queensland Dry Tropics NRM.

The sampling design for most of these programs was devel-oped to calculate suspended sediment export from the Bur-dekin River and as such samples collected were biased toward high flows, when the vast majority of annual flow is discharged. However, the data archive in the DERM pro-gram targeted baseline flows. Figure 2 shows the TSS sam-ples collected along with the temporal coverage of flow spanning 24 years of monitoring at the Inkerman Bridge site on the Burdekin catchment.

[10] While TSS analysis was performed at a number of laboratories, the same standard method was applied. Sam-ples were filtered through preweighed filter membranes, oven-dried and reweighed to determine the dry TSS weight as described by *American Public Health Association* [2005]. TSS (in mg L^{-1}) was calculated by dividing the mass of the retained matter (in mg) by the volume of sam-ple filtered (in L).

[11] Figure 3 shows the bias incurred from the sampling of concentration and flow for the Inkerman Bridge site on the Burdekin catchment. The relative bias in concentration was calculated by dividing the average flow recorded at concentration samples by the average flow recorded at reg-ular time intervals. Note, if there are gaps in flow, the flow record will need to be infilled to a regular time series using a Hermite spline interpolation [*Fritsch and Carlson*, 1980] or equivalent. Similarly, the relative bias in flow was obtained by dividing the average observed flow by the av-erage regularized flow. Since the flow was continuously measured the bias between predicted and observed flows was 1 (and thus no bias). Concentration however, is meas-ured at irregular intervals with relative biases varying
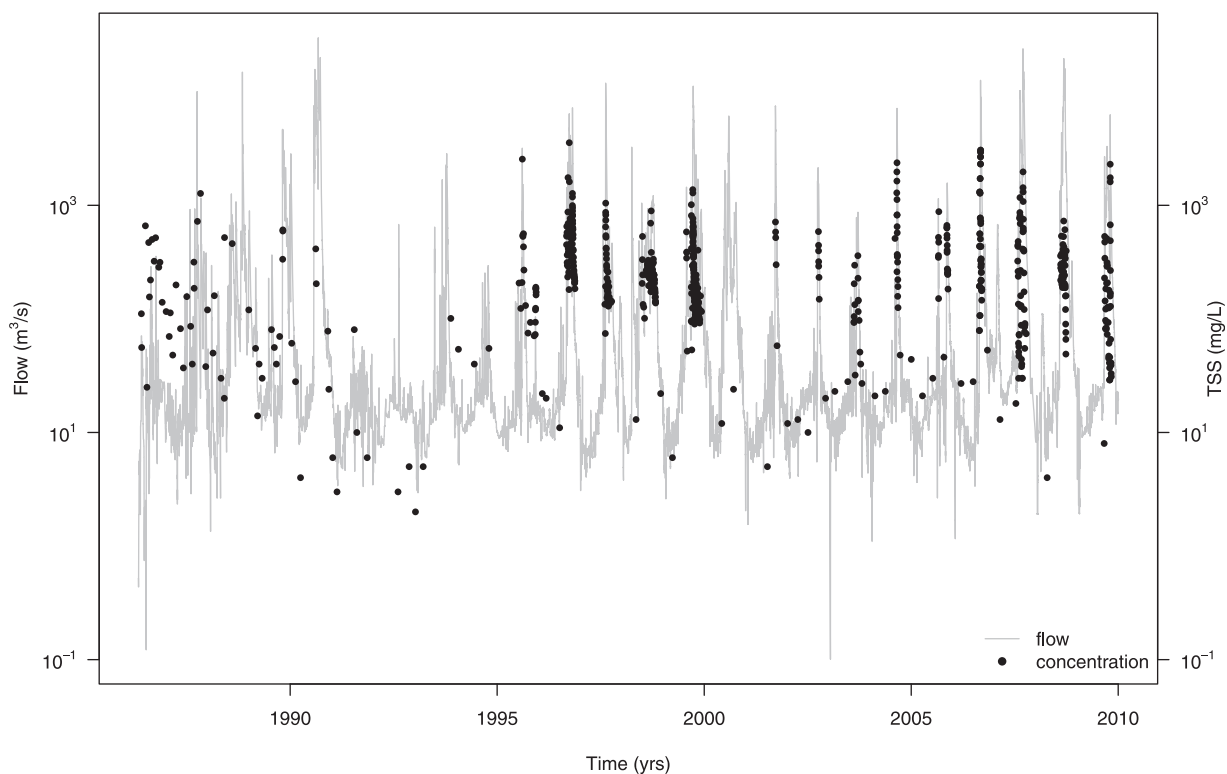

Figure 2. Observed flow (gray line) overlaid with TSS samples (points) showing the temporal coverage of data collected at Burdekin River at Inkerman Bridge between 1 October 1986 and 30 September 2010.
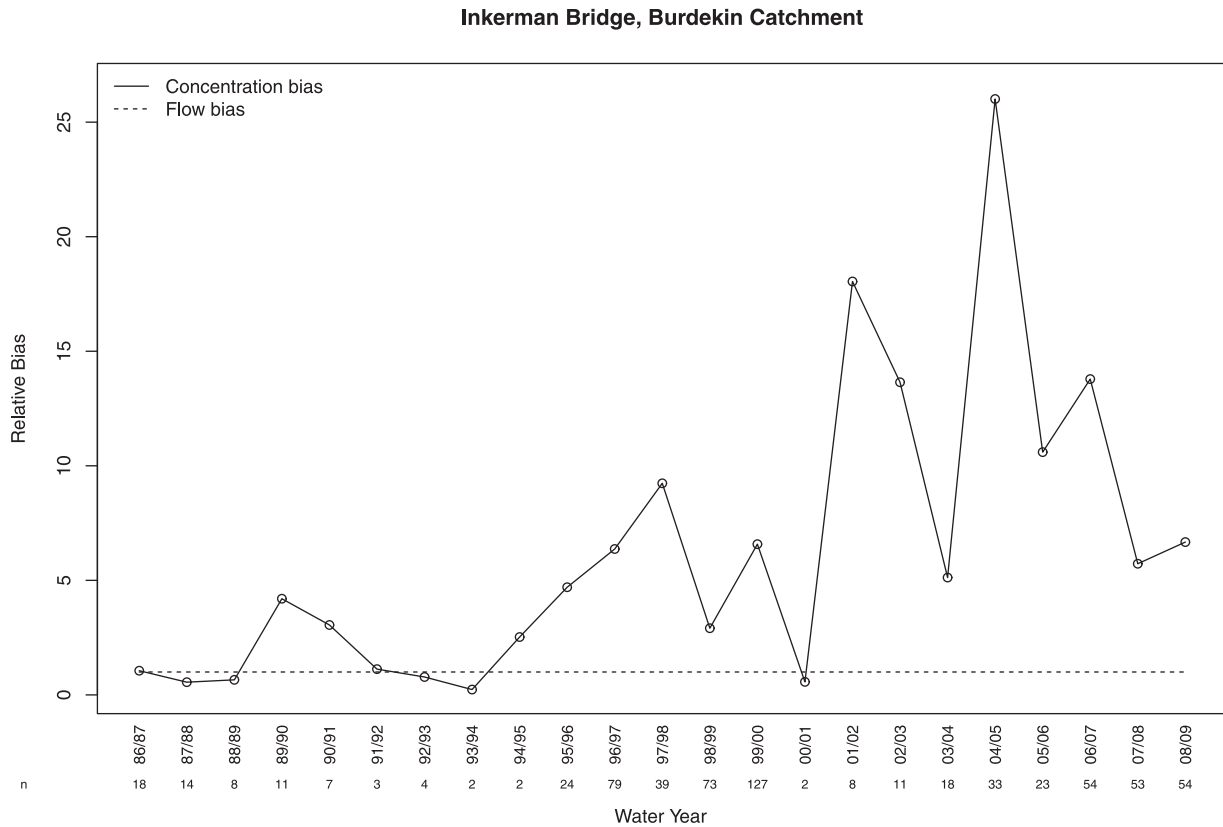
Inkerman Bridge, Burdekin Catchment

Figure 3. Summary of biases in flow (dashed line) and concentration (solid line) in TSS across water years for the Inkerman Bridge site in the Burdekin from 1973 to 2009. Sample sizes for each water year are shown beneath the *x* axis labels. Values above and below 1 indicate biases upward and downward, respectively.

between 0.01 and 26 across all water years, indicating substantial bias in concentration sampling, particularly during the later years where monitoring was restricted to high-flow discharge events only.

3. Quantifying Loads in the Burdekin River

[12] The LRE is built around a four-step process consisting of estimation steps for flow, estimation steps for concentration, estimation of the load including evaluation of model structure and calculation of the variance that incorporates errors in both concentration and flow [*Wang et al.*, 2011]. As flow at the Inkerman Bridge site is measured at regular intervals (hourly) from the Clare gauge (120006B) 15 river km upstream of Inkerman Bridge, no interpolation of the flow record is necessary and we concentrate on estimation steps for concentration and the corresponding load and variance estimates. Furthermore, we focus on the extensions of the LRE that are applicable for the case study presented.

3.1. A Predictive Model for Concentration

[13] The LRE methodology fits a GAM [*Wood*, 2006] to concentration (on the log scale) over the duration of the monitoring data. The model incorporates key hydrological processes of a river system (some of which are highlighted by *Morehead et al.* [2003]), through terms created from flow data with the aim of reducing the unexplained variance. The GAM introduces flexibility into the model by way of temporally smooth terms that are driven by the data.

[14] The GAM is composed of two components. The first includes terms that enter into the model linearly, while the second incorporates flexible (smooth) terms driven by the data. The model is considered semiparametric because of the inclusion of smooth terms in the model (second summation) and is represented mathematically as

$$\log(c_i) = \beta_0 + \sum_{k=1}^{p} \beta_k x_{ki} + \sum_{k=1}^{m} s_k(z_{ki}) + \varepsilon_i \qquad (1)$$

where x_{ki} and z_{ki} are covariates measured at the ith sample and $s_k(\cdot)$ represents a spline that fits a flexible function to the data. The basic suite of terms we consider in any base model include linear (x_{1i}) and quadratic terms (x_{2i}) for flow, to capture nonlinearity in the relationship between flow and concentration; a rising or falling limb term (x_{3i}), represented by a categorical variable that reflects concentration differences between the rising ($+1$), falling (-1) or stable (0) sections of hydrograph cover of an event; a cyclic term (z_{1i}) that captures seasonal effects throughout a water year; and a smooth discounting term (z_{2i}) that represents the effect of recent prior flow volume on concentration as an attempt to mimic exhaustion and hysteresis properties of the hydrological system. These base terms are

all described by *Wang et al.* [2011]. Although arbitrary trend terms could be explored [*Wang et al.*, 2011] and these often explain considerable amounts of unexplained variation in the data, we suggest they be omitted from the analysis and include only terms that have a direct interpretation. That is, terms that could be interpreted easily by managers (e.g., changes to vegetation, land use and land structure) and therefore be used to determine necessary changes to the landscape that may reduce loads.

[15] In developing a predictive model for the Burdekin end of river site, we begin with the suite of base terms highlighted by *Wang et al.* [2011] and identify those terms important in describing the relationship between concentration and flow, which lead to the final predictive model. Although these terms have been described elsewhere [*Wang et al.* 2011], we provide a brief description of their meaning in the context of the case study presented here for ease of interpretation and highlight differences to the *Wang et al.* [2011] implementation where necessary.

3.1.1. Linear and Quadratic Terms for Flow

[16] The relationship between concentration and flow on the log scale is often linear or quadratic in terms of its shape and has been explored in the literature [*Belperio*, 1979; *Cohn*, 1995; *Cohn et al.*, 1992]. Figure 4 shows the relationship between TSS concentration and flow (log scale) for 692 samples taken at the Inkerman Bridge site on the Burdekin River. A loess smoother is overlaid to highlight linear and quadratic features of the relationship between

concentration and flow, showing more than 2 orders of magnitude (log units) increase in concentration as the size of the flow increases. Inclusion of a quadratic term for flow in the model is therefore important.

3.1.2. Rising-Falling Limb

[17] The rising and falling limbs are periods of increase or decrease of flow over time during an event. The movement of concentration can behave differently during these flow stages and can be higher on either the rise or the fall, the nature and timing of the event and hydrological characteristics of the catchment [e.g., *Nistor and Church*, 2005; *Morehead et al.*, 2003]. Larger events have the capacity to move higher TSS concentrations, and can display more systematic concentration differences between rising and falling limbs (Figure 5). Therefore, we represent rising-falling limb behavior for events peaking above the 90th percentile flow in each water year, as shown in Figure 6a. On average, at the Burdekin site 67% of flow volume occurred above the 90th percentile in each water year. The 90th percentile, q^{90} is used as a trigger for the rising-falling limb term, x_{5i} which is a categorical variable as shown in equation (2) that indicates flow on the rise $(+1)$, fall (-1) or flat (0), where the latter may also be an indication of base flow conditions. Figure 6b shows the resulting contribution of TSS concentration for the Inkerman Bridge site (estimate and 95% confidence intervals) from samples located on the rise or fall of an event in the Burdekin River and indicates a lack of significance as both bars cross the baseline at 1. Although this
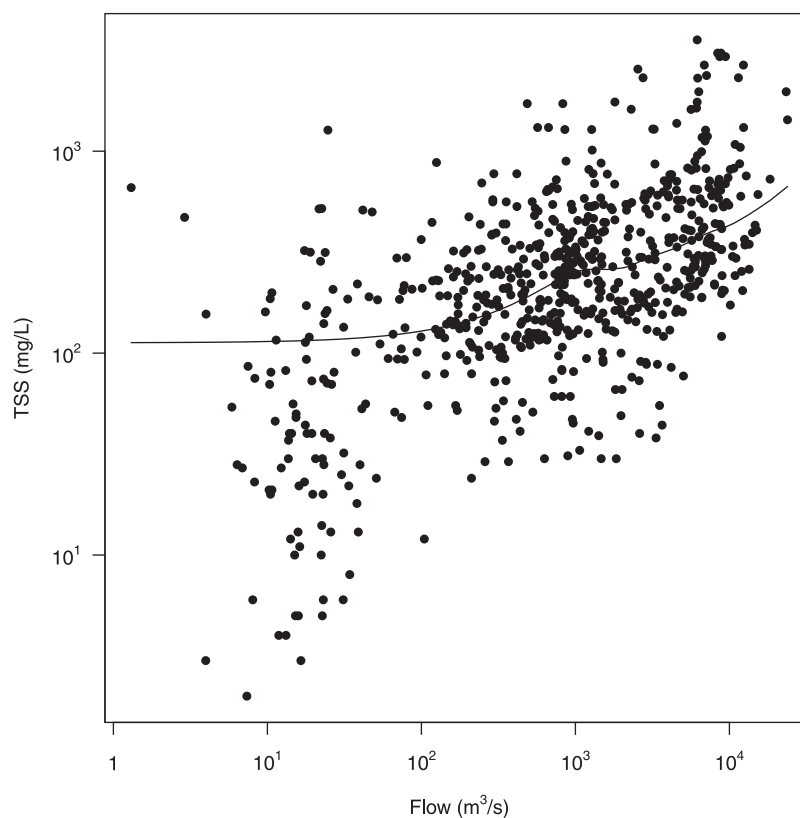

Figure 4. Relationship between TSS and flow for the Burdekin site at Inkerman Bridge with a loess smoother overlaid across the points.
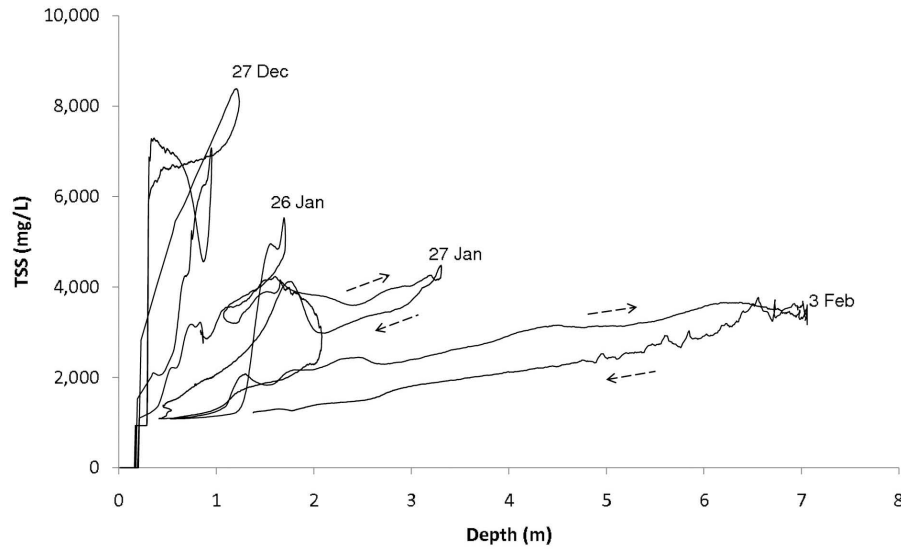
Figure 5.   Total suspended solid concentration as estimated by a turbidity probe calibrated to measured concentrations, plotted against flow depth, for the Bowen River at Myuna, a tributary of the Burdekin River (location shown in Figure 1). The event peak concentrations declined through the wet season, suggesting decline or exhaustion of sediment availability. In events above the 2 m stage, concentration was consistently higher on the rising limb than on the falling limb.

term can be important in a baseline model for many river systems, for the Burdekin, it is shown to be insignificant.

$$
x_{3i} = \begin{cases} 1 & \text{if } \hat{q}_i > \hat{q}_{i-1} \text{ and } q_i > q^{[90]} \\ -1 & \text{if } \hat{q}_i < \hat{q}_{i-1} \text{ and } q_i > q^{[90]} \\ 0 & \text{otherwise} \end{cases} \qquad (2)
$$

3.1.3.   Cyclic Seasonal Terms

[18]   Intra-annual variations in concentration can be important aspects of behavior in many climate zones, including tropical rivers like the Burdekin River. Here, tropical weather systems are prevalent during summer months, producing heavy rainfall that causes sediment erosion and transport through the watershed, resulting in the bulk of annual suspended sediment export to the GBR lagoon. We fit a seasonal term using a cyclic cubic regression spline to ensure that a smooth function of time fit across the year does not change discontinuously at the end of the year [*Wood*, 2006]. Note, this is a different representation to that used by *Wang et al.* [2011] that is more flexible, allowing the data to define the peaks and troughs through seasons. The cyclic spline was achieved by positioning 10 spline knots (locations in time where a change in concentration is likely to occur), equally spaced across the 12 months of the year to estimate the contribution of the seasonal term in the GAM as shown in Figure 7 using data from the Inkerman Bridge site. Peaks in TSS concentration are noted for November–December and April–May with declines noted between July–September. The decline from December to February occurs during the wet season when the majority of large events occur. This indicates dilution of concentration by volume of water, and/or exhaustion of the sediment supply from within the catchment. Concentrations in the Bowen River tributary of the Burdekin River also illustrate

such a decline during the middle of the wet season (Figure 5). Inclusion of such a term in the final model for concentration is therefore advantageous.

3.1.4.   Smooth Discounted Flow

[19]   The discounted flow term z_{2i} represents a simple exponential weighting of flow history designed to allow the recent prior flow volume to influence concentration predictions. The term is expressed as

$$
\begin{aligned}
z_{2_i} &= s\{\log{[y_i(\delta)]}\}, \\
\gamma_i(\delta) &= d\kappa_{i-1} + (1-\delta)\hat{q}_{i-1},
\end{aligned} \qquad (3)
$$

and $\kappa_i = \sum_{m=1}^{i} \hat{q}_m$ for discount factor δ, where κ_i represents the cumulative flow up to the ith day. As the discount variable δ approaches 1, the discounting term, γ becomes a cumulative summation of flow over the entire monitoring period. Conversely, as δ approaches 0, γ mimics the original flow time series. Choosing a value for δ between 0 and 1 therefore produces a discounting term that represents a mixture of the original flow series and a cumulative one, where δ represents the level of mixing or smoothing between the two (Figure 8). Including more than one discounting term in the model can therefore capture complex processes like hysteresis between events, where the movement of concentration at a particular point in time is related to past events and therefore exhibits a lag, for example, higher concentrations occurring following a dry period. The movement of concentration can also be affected by periods of exhaustion, where multiple large events reduce TSS availability into the system. Table 1 presents a range of discounting levels and shows that as the discount decreases, past events have little bearing on the current event. Figure 9 shows the contribution of four discounting
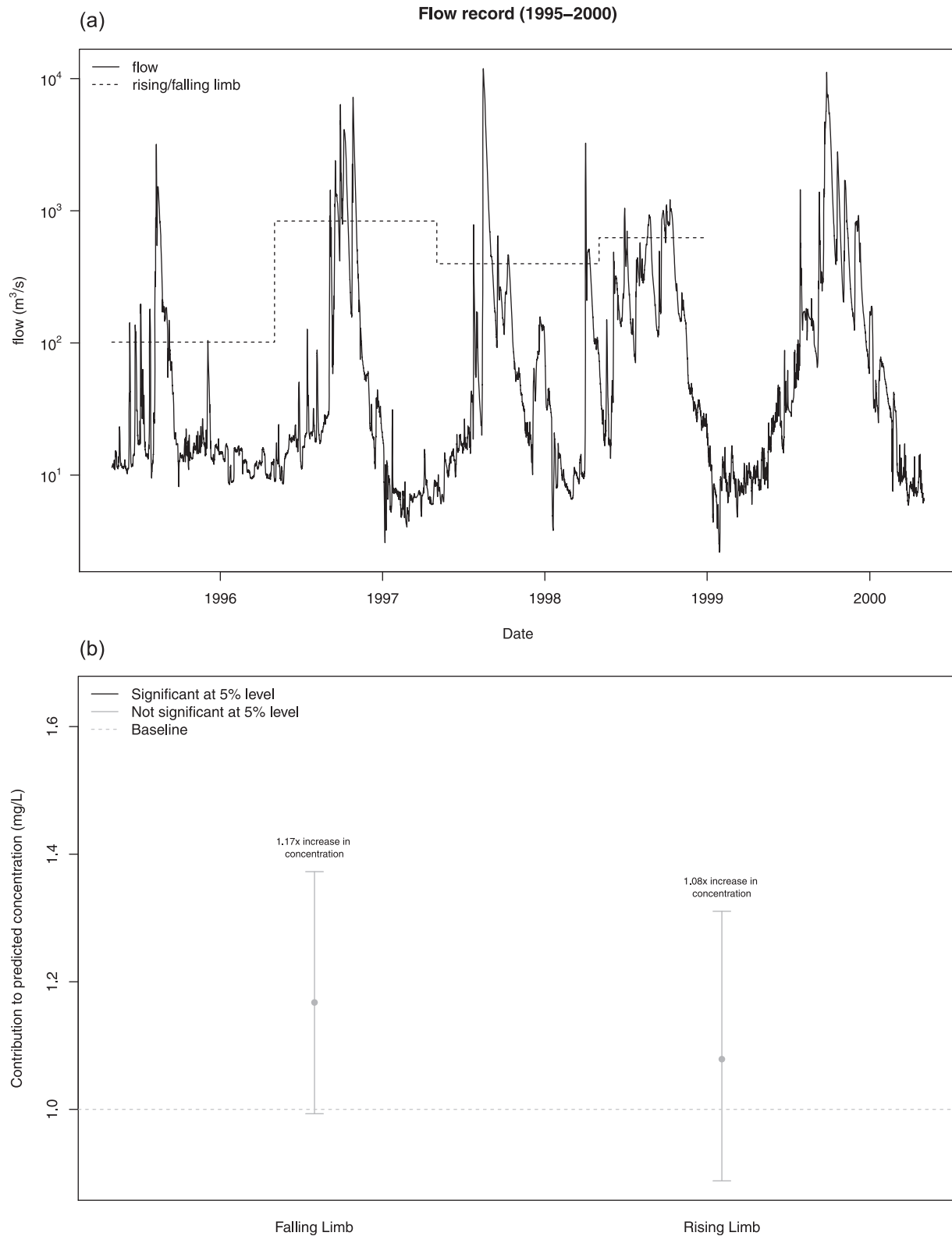
(a)

Figure 6. Construction of the rising-falling limb term and its contribution to sediment concentration in the loads regression estimator (LRE) model. (a) The rising-falling limb overlayed on top of a flow record (log scale) based on a 90th percentile cutoff determined for each water year between 1995 and 2000 to capture large events. (b) The estimated contribution (circles) of concentration from the fall or rise of an event with 95% confidence intervals. Baseline levels are indicated by a dashed gray line drawn at 1. Levels of increase or decrease are reported at the top of each bar.
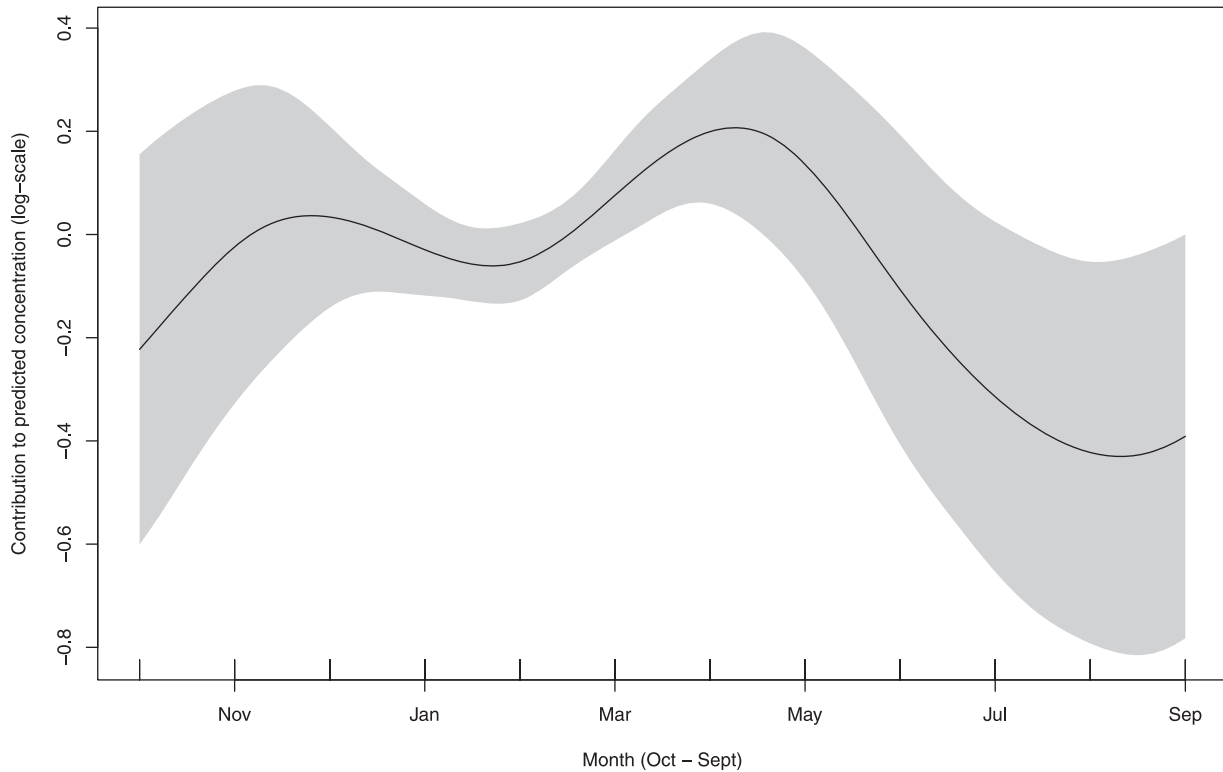
Figure 7.   Seasonal term with 95% confidence intervals (shaded) showing the variation in TSS concentration (log scale) over a water year (October–September) at the Inkerman Bridge site in the Burdekin River.

terms fit in the one model for TSS concentration at the Inkerman Bridge site in the Burdekin River. In Figure 9a for example, TSS concentration increases linearly with increasing flow assuming a small flow discounting term. However, as $\delta \rightarrow 1$, flow accumulates producing a decrease in predicted TSS concentration at high flow (Figure 9d). The inclusion of more than one discounting term may therefore be appropriate and should be tested in the model. For the Burdekin model, all four terms were included.

3.1.5.   Additional Covariates

[20]   As is often the case, the base model may not be sufficient for every type of river system encountered, particularly if multiple years are being examined. Complex relationships may exist, particularly in variable river systems like the Burdekin where drought breaking years are not uncommon. In these instances, additional terms need to be investigated to explain the temporal variations in concentration. These variables may represent additional terms extracted from the hydrograph such as the rate of change (representing a surrogate for the rainfall intensity), or pollutant sources (e.g., total flow or proportion of flow arising from subcatchments), spatial structures (e.g., a dam) or terms that capture antecedent conditions and possible management intervention (e.g., ground cover and vegetation). Although the inclusion of such terms may only explain a small proportion of the variance in a model, their input can be valuable because of their ability to explain complex processes.

[21]   To accommodate the complex features inherent in variable river systems like the Burdekin, we incorporated two additional covariates. The first of these investigated the ratio of flow from above and below the Burdekin Falls Dam, as the contributions from various subcatchments in the Burdekin can lead to considerably different suspended sediment loads because of different geology and soil types, stream and catchment characteristics (e.g., slope, bank heights, vegetation types, gully density, etc.), and the effect of the dam on trapping sediment from upstream. We obtained hourly flow data from the Burdekin River at Hydro site (gauge 120015A) which represents the flow contribution from the catchment area (115,000 km^2) above the Burdekin Falls Dam. We computed the ratio of this flow with the total flow occurring at the Burdekin River at Clare gauge, which represents the end-of-catchment site. This ratio is sometimes greater than 1 as some water is lost because of water offtake for irrigation in the lower Burdekin sugarcane industry during the relatively dry water years.

[22]   The second covariate considered was dry-season vegetation cover for the catchment as it is well known that poor vegetation ground cover can lead to an increase in soil erosion [*McIvor et al.*, 1995; *Scanlan et al.*, 1996] and therefore an increase in TSS loads. Vegetation ground cover data (*Scarth et al.* [2006]), in the form of an annual (end of dry season) ground cover index (GCI) for 52 subcatchments of the Burdekin were obtained from the Department of Environment and Resource Management (Queensland Remote Sensing Centre). The GCI estimates the percentage of plant material (dead or alive) that is covering underlying soil or rock material, through a known statistical relationship between measurements of cover made by satellite sensors calibrated to
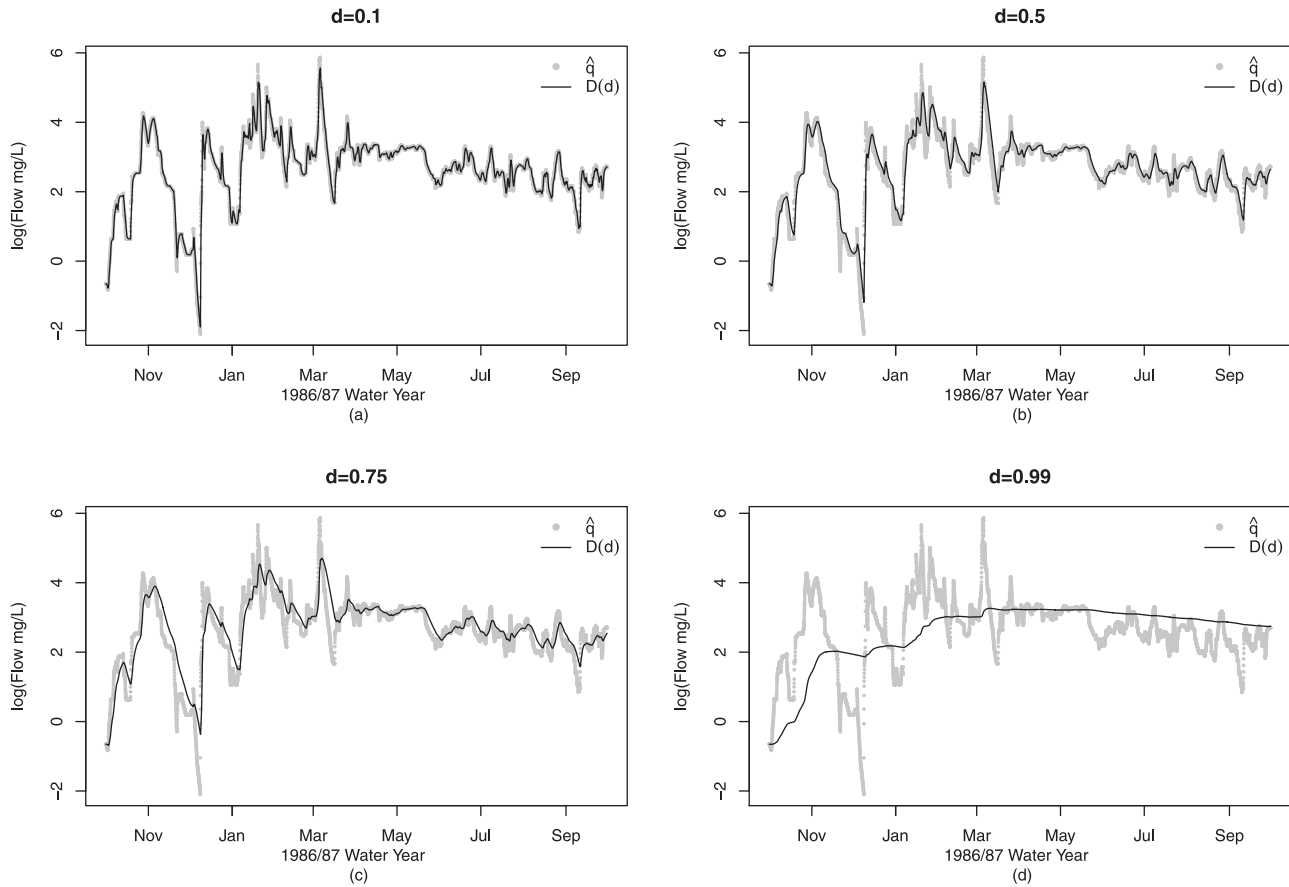
Figure 8. Illustration of different levels of discounting of flow, $\hat{q}$ for a sample water year (1986/1987) collected at Inkerman Bridge in the Burdekin River using discounts of (a) $\delta = 0.1$ (equivalent to the original flow), (b) $\delta = 0.5$ (minimal smoothing), (c) $\delta = 0.75$ (moderate smoothing), and (d) $\delta = 0.99$ (equivalent to the cumulative flow over the water year). The discounted term $\gamma(\delta)$ is overlaid as a black line.

field-based observations [*Schmidt et al.*, 2010]. We extracted the median GCI value across the Burdekin catchment for each year of the study period to be used as an input into the model.

3.2. A Model for Inkerman Bridge

[23] We fitted the base LRE model to data from the Inkerman Bridge site on the Burdekin River and investigated significant model terms using backward elimination. Additional discounting terms and covariates consisting of a vegetation term and the contribution of flow from above the dam were fit after the base model was identified and their significance was evaluated using the generalized cross-validation criterion (GCV) and p values for each term. Terms were

Table 1. Summary of Discounting Values Used in the Exponential Weighting of Flow History That Can Be Chosen to Reflect How Much Weight of the Current Flow Is due to Flows That Occurred in the Past

Discount Percent	Days Until 50% of Weight of Current	Days Until 5% of Weight of Current
99%	69	>100
95%	14	59
90%	7	29
75%	3	11
50%	1	5

eliminated that had the largest p value and therefore, decreased the GCV. The GCV is a criterion similar to ordinary cross validation but with better computational properties. It is used in this instance to evaluate the performance of spline-based terms in a GAM to identify the optimal set of knots and therefore the level of smoothness required to achieve a good fit without creating a model that is too complex.

[24] Diagnostics were then examined to determine the fit of the model and whether there were any serious departures from normality. Among the standard diagnostics, we examined stationarity. That is, whether the residuals were autocorrelated and if present, we refitted the model with an AR1 term to capture the correlation between sampling times (i.e., how much of the concentration at time t is related to the concentration measured at $t - 1$) using generalized least squares [*Pinheiro and Bates*, 2000] and estimated the variance-covariance matrix accordingly. The LRE model was fit using the R programming language [*R Development Core Team*, 2005], making use of the mgcv [*Wood*, 2006] and nlme [*Venables and Ripley*, 1998] packages. Details regarding the code can be obtained from the first author.

[25] The values of each term in the final model, which explained approximately 71% of the variation in the data are shown in Table 2 and include linear and quadratic terms for flow, vegetation cover, the ratio of flow above the dam,
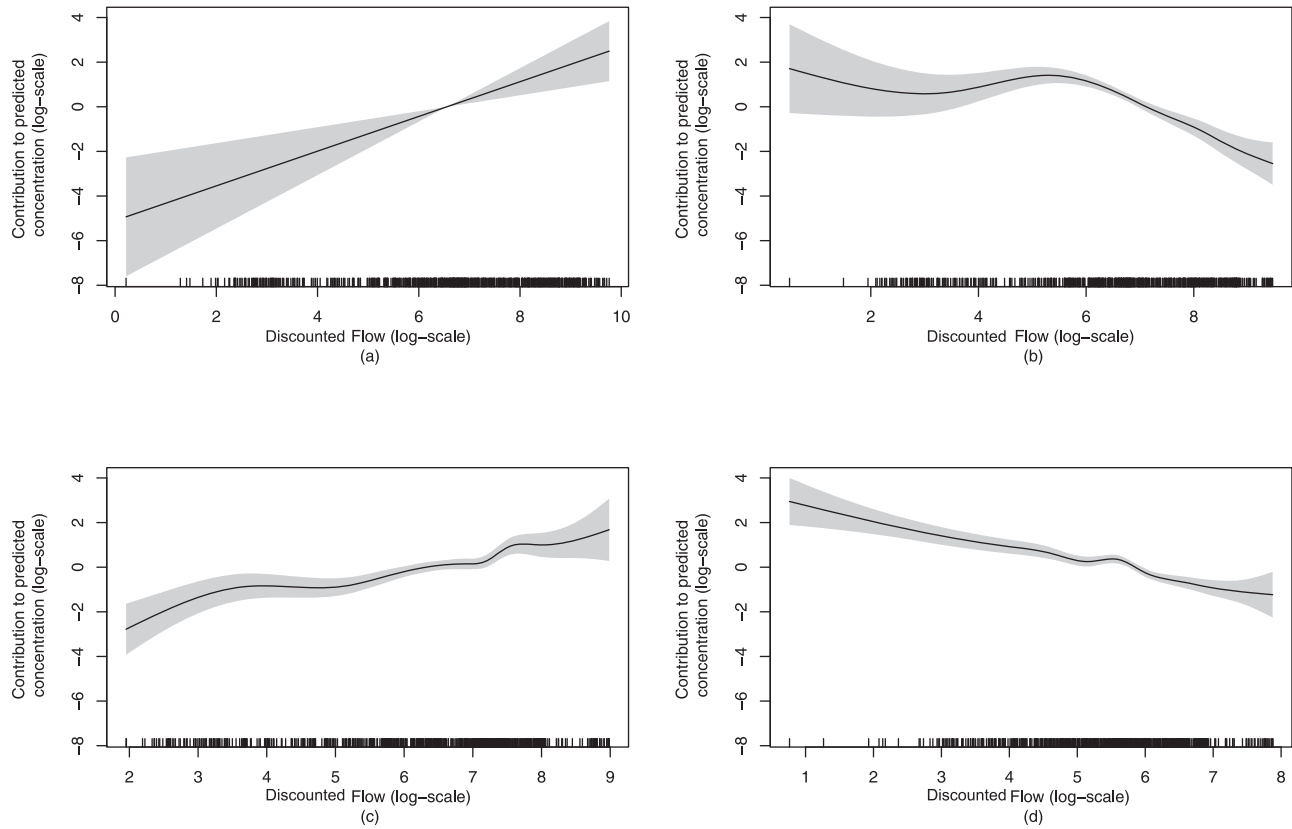
Figure 9. Smooth discounting terms fit to TSS concentrations (log-scale) at the Inkerman Bridge site in the Burdekin River computed for (a) $\delta = 0.1$, (b) $\delta = 0.75$, (c) $\delta = 0.95$, and (d) $\delta = 0.99$. Shaded regions in each figure indicated 95% confidence bounds on the estimates. A rug plot is shown at the base of each plot to indicate the distribution of data available.

a seasonal term and multiple discounting terms to capture hydrological features of the system. In this example, the correlation estimated from the autoregressive process is estimated to be 0.97, indicating quite strong correlation between concentration measurements taken from one time

Table 2. Parameter Estimates for the Fixed Effects, Smooth Terms, and Correlation Term Resulting From the Fitted Loads Regression Estimator (LRE) Model to the Inkerman Bridge Site in the Burdekin Catchment

Parameter	Estimate	Standard Error	p value
Intercept	12.280	1.195	<0.001
Log(flow)			
Linear	−1.464	0.249	<0.001
Quadratic	0.111	0.014	<0.001
Vegetation cover	−0.021	0.003	<0.001
Ratio of flow above dam	−0.977	0.186	<0.001

Smooth Terms	Effective Degrees of Freedom	p value
Seasonal		
s(month)	4.252	0.014
Discounting terms		
$s(d = 0.1)$	1.001	<0.001
$s(d = 0.75)$	6.073	<0.001
$s(d = 0.95)$	8.763	<0.001
$s(d = 0.99)$	8.035	<0.001
Correlation (AR1(ϕ))	0.9723	

point to another. As the rising-falling limb term was not significant (p value >0.05) it was therefore not included in the final model. Table 3 shows a subset of models explored before identifying the optimal model. Model 1 fits all the terms in the model, while models 2–4 represent additional fits from a backward elimination that omits the term that contributes the least in terms of the percent variation explained and GCV value. These models are compared with the *Wang et al.* [2011] model (model 5) and a simple representation of concentration and flow (model 6). The results indicate the large contributions made by the inclusion of the hydrological terms outlined in *Wang et al.* [2011] (17.5%) and the inclusion of additional discounting terms (12.1%) introduced in this paper. The addition of vegetation cover and the contribution of flow from upstream sites provide an additional 4%.

[26] Of major interest in this model are the two additional covariates. The inclusion of vegetation cover indicated a significant decrease in TSS concentration as vegetation cover increases (i.e., 2.1% decrease per percentage increase in vegetation cover). Furthermore, for every unit increase in flow above the dam, we observe a significant decrease in TSS concentration (up to 38%). Although the inclusion of these terms explains only an additional 4% of the variation, they provide an explanation of the decrease in loads observed during the 1996/1997 and 1997/1998 water years, when consistent high volumes of flow entered the system but a much smaller load resulted in the latter of the two years. Similarly,

Table 3. Comparison of a Subset of Models Fit to the Inkerman Bridge Site, Burdekin River[a]

Model	Explanation	GCV	Percent Variation Explained	Percent Contribution
1. Intercept + flow terms + limb + seasonal + flow discount terms + vegetation cover + ratio of flow above dam	Base model (5) + additional discounting terms and covariates	0.409	71.3%	0.2%
2. Intercept + flow terms + seasonal + flow discount terms + vegetation cover + ratio of flow above dam	Model 1 − limb	0.409	71.1%	2.0%
3. Intercept + flow terms + seasonal + flow discount terms + ratio of flow above dam	Model 1 − limb − vegetation cover	0.445	69.1%	2.0%
4. Intercept + flow terms + seasonal + flow discount terms	Model 1 − limb − vegetation cover − ratio of flow above dam	0.472	67.1%	12.1%
5. Intercept + flow terms + limb + seasonal + flow discount term	Base model [*Wang et al.*, 2011]	0.607	55.0%	17.5%
6. Intercept + flow terms	Simple flow representation	0.808	37.5%	−

[a]Each model is accompanied by the generalized cross-validation (GCV) score, the percentage of variance explained by the model, and the percent contribution from the inclusion or exclusion of particular terms in each model. Model 2 is the final model used.

the load estimated in the 2008/2009 water year was 27% lower when compared to the load estimated in 2007/2008 despite the annual flows being within 6%.

[27] An interesting feature in Figure 10b is a possible cyclic pattern observed in the annual mean concentration, showing higher TSS loads in 1987/1988, 1996/1997, 2004/2005 and 2005/2006. Although we could not explicitly explain the higher loads during these periods with specific climatic terms in the model e.g., effects due to El Niño or La Niña cycles, it was hypothesized that major cyclones crossing the North Queensland coast, affecting areas around Innisfail (1986, 2006: Tropical Cyclones Winifred and Larry), Bowen (1988: Tropical Cyclone Charlie), Cairns/Townsville (1997: Tropical Cyclone Justin) (Bureau of Meteorology, Previous tropical cyclones, http://www.bom.gov.au/cyclone/history/index.shtml2011) and therefore impacting on the Burdekin catchment, could be the main contributor.

3.3. Estimating the Load and Quantifying the Variance

[28] The estimation of load in each water year involves multiplying the flow measured at regular time intervals by the concentration predicted at each regularized flow value and then summing over the water year. An expression of the load in any one water year is

$$\hat{L} = K \sum_{m=1}^{M} \hat{c}_m \hat{q}_m \exp(\sigma_m) \tag{4}$$

where K is a unit conversion constant for producing a load in tons given concentration is measured in milligrams per liter (mg L^{-1}) for TSS and flow is measured in cubic meters per second, $\hat{q}_m$ and $\hat{c}_m$ represent predicted regularized flow and concentration at regular time, m, and $\exp(\sigma_m)$ represents the standard bias correction term for operating on the log scale. See *Wang et al.* [2011] for details.

[29] The expression shown in equation (5) incorporates errors in the flow rates that the user can provide in the form of a coefficient of variation, α_1 and α_2 [*Wang et al.* 2011].

$$\text{var}(\hat{L}|\hat{C}, \hat{Q}) = \text{trace}\{\text{var}(\hat{\beta})X^T P P^T X\}$$
$$+ \alpha_1^2 \sum_m \hat{l}_m^2 \{1 + \partial f / \partial \log \hat{q}_m\}^2 + \alpha_2^2 \{1 + \partial f / \partial \log \hat{q}_m\}^2 \tag{5}$$

For completeness, we outline the components of the variance expression. In equation (5), $P = (\hat{l}_1, \hat{l}_2, \ldots, \hat{l}_M)$, represents a vector of loads estimated for each regular time

interval, m, $\hat{l}_m = K\hat{c}_m\hat{q}_m \exp(\sigma_m)$ and $f(\hat{Q}) = \beta X$, where M represents the maximum number of time intervals. The second term in equation (5) represents an error due to the spatial positioning of the gauge, while the third term represents a relative measurement error in the flow rate. A brief summary of the variance calculation is provided by *Wang et al.* [2011], however, the complete derivation of this expression is contained in the auxiliary material.[1] The calculation of the $(1 - \alpha)$% confidence intervals can then be achieved in the usual way by taking $\exp\left(\hat{L} \pm v_{\alpha/2}\sqrt{\text{var}(\hat{L})}\right)$ where α represents the significance value that you wish to attain and $v_{\alpha/2}$ represents the percentage point from a normal distribution for a given level of significance.

[30] The loads methodology produces a total load, in tons, for each water year. To facilitate the comparison of loads through time a method of standardizing the load to provide an annual flow-weighted mean concentration is required. We derive the flow-weighted concentration along with an expression of the variance.

[31] Let $\hat{L}_w$ represent the load in millions of tons calculated for a water year, w using the expression shown in equation (5) and let $\hat{F}_w$ represent the total volume of flow in mega liters occurring in a water year. We constructed an annual flow-weighted mean concentration, A_w by dividing the total load by the total volume of flow and multiplying by the necessary constant λ to obtain a result in mg L^{-1},

$$A_w = \lambda \hat{L}_w / \hat{F}_w \tag{6}$$

with corresponding variance

$$\text{Var}(A_w) = \frac{\lambda^2}{\hat{F}_w^2} \text{Var}(\hat{L}_w) \tag{7}$$

Confidence intervals can be computed accordingly

[32] The resulting estimates of loads are shown in Figure 10 and Table 4. Figure 10a shows the TSS load estimates (squares) and 80% confidence intervals for each water year, accompanied by the total volume of flow observed in that water year as a bar plot to the right. Annual flow weighted mean concentrations and associated 80% confidence intervals are shown in Figure 10b.

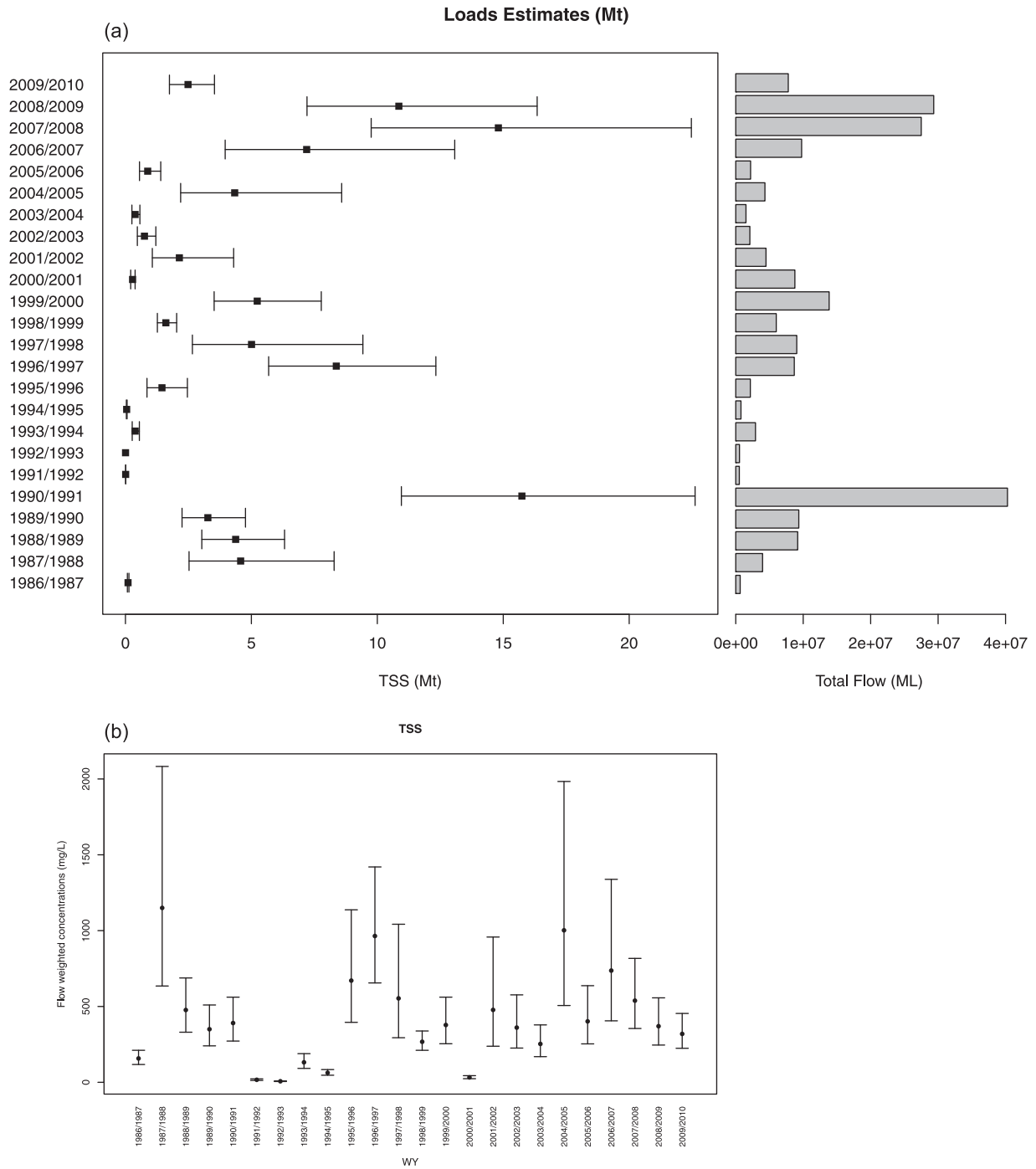[1]Auxiliary materials are available in the HTML. doi:10.1029/2011WR011080.

Figure 10.   A summary of model estimates from fitting the LRE model to the Inkerman Bridge site in the Burdekin River showing (a) estimated TSS loads (Mt) and 80% confidence intervals produced for each water year with a corresponding bar plot showing the total volume of flow to the right and (b) the annual mean concentration (mg L^{-1}) and associated 80% confidence intervals.

[33] As a secondary analysis, we also recalculated the load estimates assuming errors in the flow rates; in particular, a 10%, 30% and 50% error related to the spatial positioning of the gauge and the measurement of flow. As expected, the results showed no change in the best estimate of load in each water year. However, the CV of load estimates in each year increased with increasing uncertainty in flow, as expected (Figure 11).

4.   Validation of Model and Load Estimates

[34]   We used *k*-fold cross validation [*Efron and Tibshirani*, 1993], where $k = 10$ to investigate the predictive performance of the model for the Burdekin data set. Cross validation is performed by dividing the data into *k* subsets of approximately equal size, fitting the LRE model *k* times, each time leaving out one of the subsets and predicting on

Table 4. Load Estimates Produced for Each Water Year From the Inkerman Bridge Site in the Burdekin River Using LRE[a]

Water Year w	Total Flow (ML)	$\hat{L}_w$ (Mt)	SE	CV (%)	n	$\hat{L}_w^{0.1}$	$\hat{L}_w^{0.9}$	$\hat{A}_w$ (mg L^{-1})	$\hat{A}_w^{0.1}$	$\hat{A}_w^{0.9}$
1986/1987	656,326	0.103	0.02	22.9	18	0.077	0.138	157	117	211
1987/1988	3,978,072	4.574	2.12	46.4	14	2.526	8.285	1150	635	2083
1988/1989	9,181,633	4.376	1.25	28.6	8	3.032	6.317	477	330	688
1989/1990	9,348,329	3.272	0.96	29.3	10	2.247	4.766	350	240	510
1990/1991	40,289,050	15.741	4.45	28.3	6	10.955	22.617	391	272	561
1991/1992	530,578	0.009	0.00	24.4	3	0.006	0.012	16	12	22
1992/1993	554,509	0.004	0.00	19.7	4	0.003	0.005	7	5	9
1993/1994	2,927,424	0.385	0.11	28.2	2	0.269	0.553	132	92	189
1994/1995	774,658	0.048	0.01	22.9	2	0.036	0.065	63	47	84
1995/1996	2,162,926	1.450	0.60	41.2	24	0.855	2.460	671	395	1137
1996/1997	8,679,227	8.371	2.53	30.2	79	5.686	12.324	965	655	1420
1997/1998	9,045,261	5.006	2.47	49.4	39	2.658	9.427	553	294	1042
1998/1999	6,007,503	1.605	0.30	18.4	73	1.268	2.033	267	211	338
1999/2000	13,849,068	5.232	1.62	30.9	122	3.521	7.775	378	254	561
2000/2001	8,765,625	0.283	0.07	23.8	2	0.209	0.384	32	24	44
2001/2002	4,485,247	2.141	1.16	54.3	8	1.067	4.296	477	238	958
2002/2003	2,092,792	0.755	0.28	36.6	10	0.472	1.207	361	226	577
2003/2004	1,516,142	0.384	0.12	31.4	18	0.256	0.574	253	169	378
2004/2005	4,328,213	4.338	2.31	53.3	23	2.192	8.585	1002	506	1983
2005/2006	2,199,683	0.884	0.32	36.0	23	0.557	1.401	402	253	637
2006/2007	9,768,650	7.195	3.35	46.6	52	3.960	13.073	737	405	1338
2007/2008	27,502,587	14.806	4.82	32.6	53	9.757	22.469	539	355	817
2008/2009	29,352,221	10.855	3.47	31.9	52	7.208	16.346	370	246	557
2009/2010	7,787,247	2.485	0.68	27.5	47	1.747	3.535	319	224	454

[a]Each load estimate is accompanied by the total flow (ML), the standard error (SE) of the load estimate, the coefficient of variation (CV) expressed as a percentage, the sample size (n) and lower and upper bounds ($\hat{L}_w^{0.1}$ and $\hat{L}_w^{0.9}$) corresponding to an 80% confidence interval. The average mean concentration ($\hat{A}_w$) and associated 80% confidence intervals are also presented in the last three columns and are reported to the nearest mg L^{-1} since laboratory measurements are only reported to this level of precision.
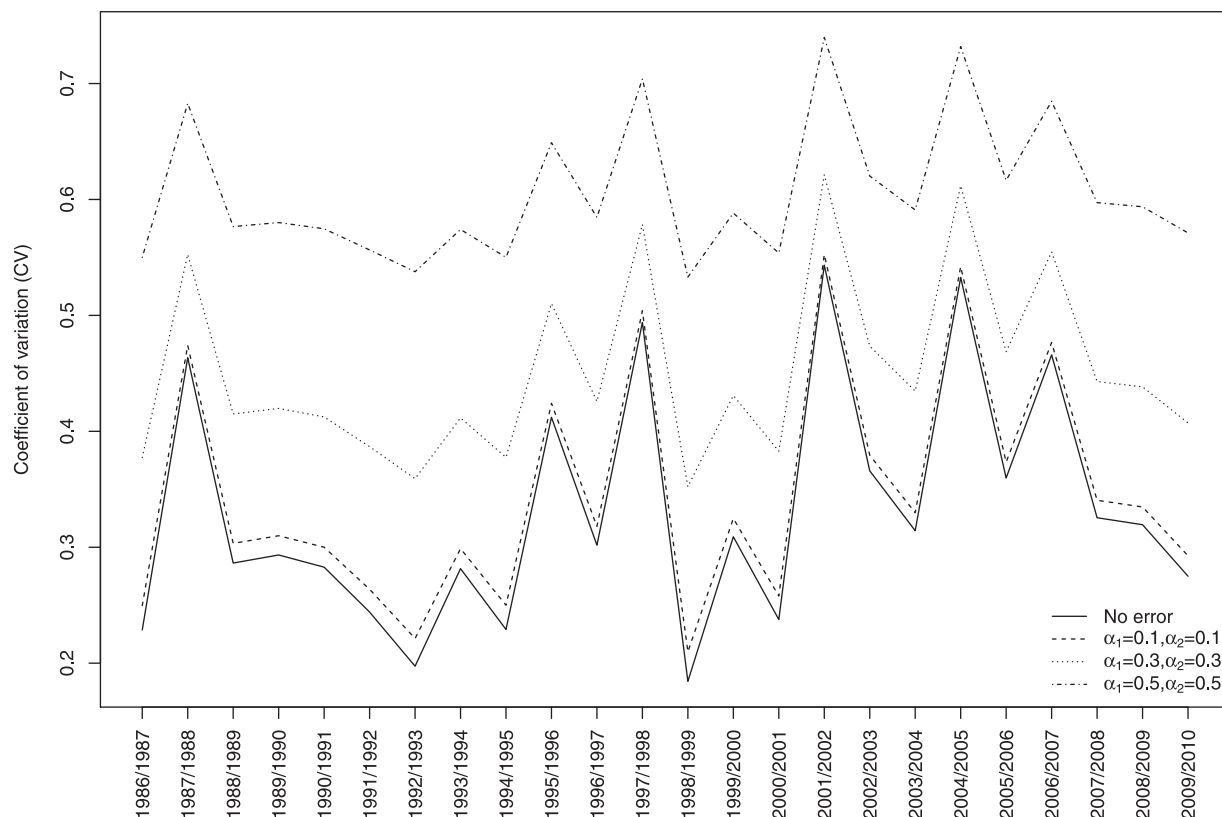

Figure 11. Coefficient of variation for the predicted loads at each water year shown for a model assuming no errors (solid line), 10% errors (dashed line), 30% errors (dotted line), and 50% errors (dot-dashed line) in the measurement and spatial location of flow gauges.

the omitted subset of data. The choice of k is typically ten-fold so as to optimize the variance-bias tradeoff with values of either 10 or 20 optimally used [*Kohavi*, 1995]. For the Burdekin case study, this involves randomly selecting observations, stratified by water year to avoid unrealistic sampling scenarios where samples occur in 1 year. The LRE model was fit to the $k - 1$ subsets of data with predictions formed on the k th subset. The approach has been shown to be superior to split-sample validation and is popular in machine learning and statistics applications for exploring the prediction error, a measure that determines how well a model predicts the response of a future observation. The prediction error is calculated as the expected squared difference between a future response and its prediction from the model [*Efron and Tibshirani*, 1993]. Therefore, if y_i represents the i th observed response and $\hat{y}_i^{-k(i)}$ represents the fitted value for the i th observation with the $k(i)$ th subset of data removed, then the cross-validated prediction error can be represented as $\mathrm{PE}^{CV} = \frac{1}{n} \sum_{i=1}^{n} \left(y_i - \hat{y}_i^{-k(i)} \right)^2$. Errors close to 0 indicate robustness of the model to unseen observations.

[35] We implemented tenfold cross validation to the Burdekin example and produced a cross-validated prediction error in observed instantaneous concentrations of 0.464, indicating low prediction error and suggesting that the model is robust to new observations. Note, this is comparable to the GCV estimate produced for the model for the complete data set (GCV = 0.409) and reflects the close relationship between predicted and observed TSS concentrations as shown in Figure 12 (i.e., points are scattered along the diagonal).

5. Discussion and Conclusions

[36] The LRE model presents a methodology for modeling concentration to provide estimates of river pollutant loads with uncertainties with application to the Inkerman Bridge site on the Burdekin River. The method's ability to capture complex characteristics of this river system provides the ability to explain the sources of concentration changes over time and how this impacts on loads.

[37] Unlike standard methods for calculating loads, such as linear interpolation, ratio estimators and rating curves, the LRE methodology contains temporally dynamic terms which provides more credible estimates compared to steady state rating curve approaches. This is true for loads over short time periods, such as individual years, and variable
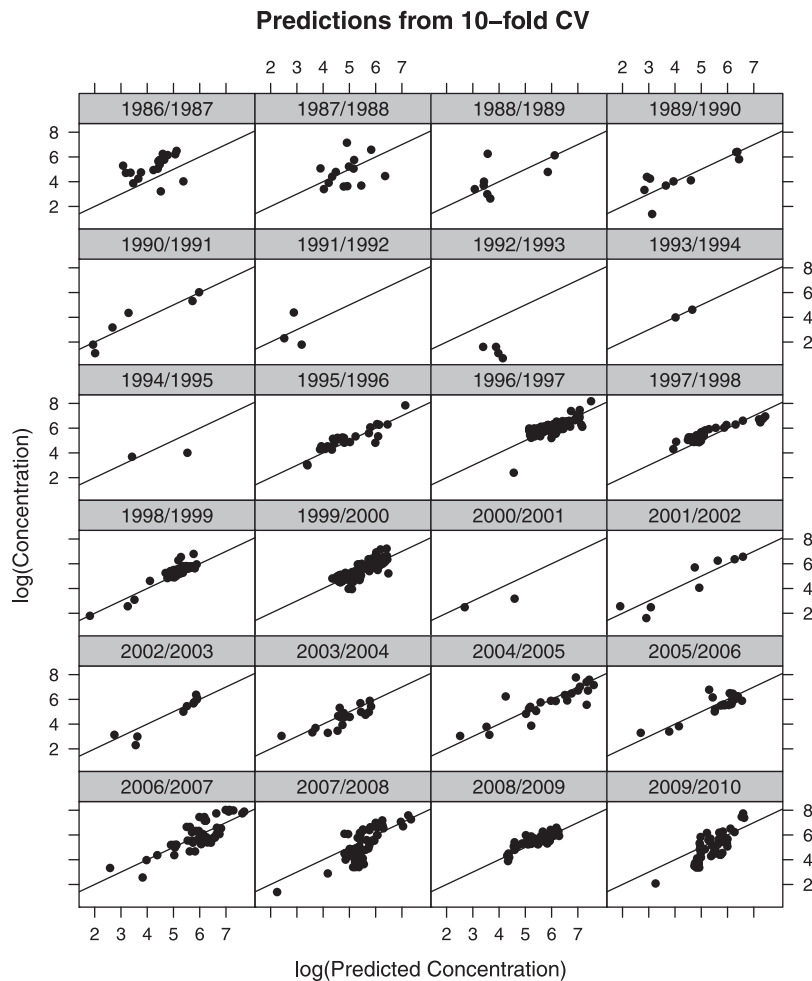

Figure 12. Results from performing tenfold cross validation showing the observed and predicted concentration in each water year.

climates where concentration is poorly predicted by flow alone. Multiple discounting terms help to represent hysteresis and exhaustion behavior evident in observed concentrations in many river systems as demonstrated by the Burdekin River. The inclusion of additional terms representing the spatial source of runoff and vegetation cover indicates that catchment conditions in 1 year influenced (reduced) the sediment load in the subsequent year. Further, the method can be applied to data independent of the sampling regime. We have also demonstrated methods for evaluating whether the terms included in the model describe the hydrological processes and adequately capture the variation and complex relationships exhibited by the system.

[38] The reliability of the model was examined through the GCV score, examination of residuals to test for stationarity and cross validation, the latter providing an estimate similar to GCV that indicates the model's ability to predict future observations accurately. The results from tenfold cross validation indicated that the model provided a reasonable fit to the data. Despite this, the load calculations in Figure 10 showed variability in loads spanning the 24 year period, with wide 80% confidence intervals for those water years exhibiting large discharges due to large rainfall events. These wide confidence intervals are the result of unexplained variation in the model. In fact, the large variations in loads and quantified uncertainties are a clear indication that the Burdekin River is a highly complex and variable river system, subjected to drought-breaking floods that lead to increases in sediment transport to the GBR lagoon [*McCulloch et al.*, 2003].

[39] Compared to the commonly used linear interpolation method, the load calculations presented by LRE are similar for the years calculated in Table 5, apart from one calculation in 2005/2006, where the linear interpolation estimate is at the lower bound the LRE 80% confidence interval. Table 5 provides some reassurance that the loads estimated by LRE are in line with standard methods but provides improved explanatory and predictive power in addition to providing confidence intervals to determine the variability in loads among years.

Table 5. Comparison of LRE and Linear Interpolation Loads Estimates for Years Spanning 1995–2000 and 2004–2010[a]

| Year | Total Discharge (10^6 ML) | TSS (10^6 t) | | LRE 80% Confidence Intervals | |
		Linear Interpolation	LRE	Lower	Upper
1995/1996	2.16	1.5	1.45	0.86	2.46
1996/1997	8.66	6.8	8.37	5.69	12.32
1997/1998	8.97	3.5	5.01	2.66	9.43
1998/1999	5.98	1.4	1.61	1.27	2.03
1999/2000	13.32	4.0	5.23	3.52	7.78
2004/2005	4.27	2.7	4.34	2.19	8.59
2005/2006	2.00	0.5	0.88	0.56	1.40
2006/2007	8.50	6.1	7.20	3.96	13.07
2007/2008	26.50	12.3	14.81	9.76	22.47
2008/2009	29.20	9.0	10.86	7.21	16.35
2009/2010	7.79	1.9	2.49	1.75	3.54

[a]Only years where linear interpolation could be applied are listed. Total discharges for each water year are also listed. TSS, total suspended sediment.

[40] The LRE methodology is unbiased by gaps in flow and concentration monitoring data as it uses a regularized flow record to predict concentration for a given regression model and to calculate the loads accordingly. In the case of the Burdekin River, flow was recorded at regular hourly intervals, but this is not the case at all sites. The regularization method currently implemented in LRE deals with small gaps efficiently using a Hermite spline interpolation. However, one limitation of the method is the interpolation of large gaps in the flow record. In these instances, the spline interpolation does not work well. *Pagendam and Welsh* [2011] have developed an approach that provides a realization of the flow series that has the potential to infill large gaps in flow data more efficiently and accurately, provided that the covariates characterizing the mean has a strong relationship with flow. The method can also provide estimates of uncertainty in the flow record that could be used to inform the errors in flows and input into the LRE model. We are currently investigating this approach as a method for flow regularization in flow records that exhibit large gaps in flow.

[41] A second limitation of the approach is the ability of the model to predict concentration and to compute an accurate estimate of the load. We included two additional terms in the model to capture some of the complex features of the concentration-flow relationship for the Burdekin River. Other more complex covariates could have been considered. For instance, instead of just breaking flow up into "above dam" and "below dam" as we do here, we could have included a much more complex breakup into, say, six flow regions based on rainfall in each of the major subcatchments: Bowen, Belyando, Suttor, upper Burdekin, Cape, and the lower Burdekin. However, the creation of these terms becomes challenging as the detailed location of major rainfall gauges is not always known and this information has marked effects on load. Of course the model is only as good as the data and covariates that are used to develop it. If the data are not representative of the system, then the calculated loads will not adequately reflect the movement of pollutants at the site. Even if we have the best data and covariates included in the model, sampling bias may still be an issue. In these instances, provided that we have covered enough of the hydrological conditions to ensure the prediction errors are minimized, the model can still be confidently used to predict concentrations and estimate loads. To facilitate this, diagnostic checks that examine the predictive performance of the model need to be performed to ensure the final model is representative of the system being studied. It is important to acknowledge that the methodology presented here is not intended to replace monitoring programs but complement them by using historical data to establish baselines against which to assess future change. Of course where significant future changes are likely, these will need to be monitored independently as they will not be represented by the model and any predictions from the model are likely to be underestimated. Furthermore, the uncertainty associated with baseline estimates may make it virtually impossible to comment scientifically on changes incurred by the implementation of management strategies. Although not an ideal outcome, this highlights the complexity of quantifying sediment fluxes.

[42] The application of the method to other water quality data sets [*Kroon et al.*, 2012] for broader management

purposes shows promise as a tool for quantifying pollutant loads with associated uncertainties. Recent examples of LRE implementation have included that of *Kroon et al.* [2012], where pollutant baseline loads were estimated for all GBR end-of-catchment sites having adequate monitoring data. Estimates of a catchment-wide sediment budget for the Burdekin is another example, where LRE methodology was used to provide estimates of loads with uncertainties for each water year from 2005–2010 for five river stations within the Burdekin catchment. These estimates were then combined and the uncertainties propagated to give sediment trapping estimates for the Burdekin Falls Dam during each year monitored by S. E. Lewis et al. (manuscript in preparation), to identify years where trapping was highest, and compare results with standard reservoir trapping algorithms developed for more temperate climates.

[43] Load estimates with attached confidence intervals from LRE are complementary to, and potentially useful for constraining, deterministic and spatially resolved models of pollutant delivery through river networks such as the Sed-Net conceptual process model of pollutant sources and transport [*Wilkinson et al.*, 2009], and land use concentration-based models of pollutant generation [*Argent et al.*, 2009]. A natural extension to the problem of loads estimation is the integration or assimilation of monitoring data with spatially resolved pollutant transport models [*Berliner*, 2003; *Wikle and Berliner*, 2007]. Through this integration, the prediction of a system's state is averaged with a new measurement about that state, thus incorporating errors in not only the state of the system but the measurement about it, in a similar way to how meteorological observations are used to improve the predictions of process-based weather models [*Kalnay*, 2003]. This is currently an area of future research, which we are exploring using the Burdekin catchment as a case study.

References

American Public Health Association (2005), *Standard methods for the examination of water and wastewaters*, 21st ed., pp. 2–56, edited by A. E. Eaton et al., Am. Public Health Assoc., Washington, D. C.

Amos, K., J. Alexander, A. Horn, G. Pocock, and C. Fielding (2004), Supply limited sediment transport in a high discharge event of the tropical Burdekin River, north Queensland, Australia, *Sedimentology*, *51*, 145–162.

Argent, R. M., J. M. Perraud, J. M. Rahman, R. B. Grayson, and G. M. Podger (2009), A new approach to water quality modelling and

environmental decision support systems, *Environ. Modell. Software*, *24*, 809–818.

Asselman, N. E. M. (2000), Fitting and interpretation of sediment rating curves, *J. Hydrol.*, *234*, 228–248.

Bainbridge, Z., S. Lewis, A. Davis, and J. Brodie (2008), Event-based community water quality monitoring in the Burdekin dry tropics region: 2007/08 wet season update, *ACTFR Rep. 08/19*, Aust. Cent. for Tropical Freshwater Res., James Cook Univ., Townsville, Queensl., Australia. [Available at http://www-public.jcu.edu.au/tropwater/reports/2007/index.htm.]

Bainbridge, Z., E. Wolanski, J. G. Álvarez-Romero, S. E. Lewis, and J. E. Brodie (2012), Fine sediment and nutrient dynamics related to particle size and floc formation in a Burdekin River flood plume, Australia., *Mar. Pollut. Bull.*, doi:10.1016/j.marpolbul.2012.01.043, in press.

Belperio, A. (1979), The combined use of wash load and bed material load rating curves for the calculation of total load: An example from the Burdekin River, Australia, *Catena*, *6*, 317–329.

Berliner, L. M. (2003), Physical-statistical modeling in geophysics, *J. Geophys. Res.*, *108*(D24), 8776, doi:10.1029/2002JD002865.

Brodie, J. E., J. Waterhouse, S. E. Lewis, A. T. Bainbridge, and J. Johnson (2009), Current loads of priority pollutants discharged from Great Barrier Reef Catchments to the Great Barrier Reef, *Rep. 09/02*, Aust. Cent. for Tropical Freshwater Res., James Cook Univ., Townsville, Queensl., Australia. [Available at http://www-public.jcu.edu.au/public/groups/everyone/documents/technical_report/jcuprd_057072.pdf.]

Brodie, J. E., F. J. Kroon, B. Schaffelke, E. C. Wolanski, S. E. Lewis, M. J. Devlin, I. C. Bohnet, Z. T. Bainbridge, J. Waterhouse, and A. M. Davis (2012), Terrestrial pollutant runoff to the Great Barrier Reef: An update of issues, priorities and management responses, *Mar. Pollut. Bull.*, doi:10.1016/j.marpolbul.2011.12.012, in press.

Cohn, T. A. (1995), Recent advances in statistical methods for the estimation of sediment and nutrient transport in rivers, U.S. Natl. Rep. Int. Union Geod. Geophys. 1991–1994, *Rev. Geophys.*, *33*, 1117–1124.

Cohn, T. A., D. L. Caulder, E. J. Gilroy, L. D. Zynjuk, and R. M. Summers (1992), The validity of a simple statistical model for estimating fluvial constituent loads: An empirical study involving nutrient loads entering Chesapeake Bay, *Water Resour. Res.*, *28*, 2353–2363.

Cooper, D. M., and C. D. Watts (2002), A comparison of river load estimation techniques: Application to dissolved organic carbon, *Environmetrics*, *13*, 733–750.

Darnell, R., B. Henderson, F. Kroon, and P. Kuhnert (2012), Determining the number of years of monitoring pollutant loads necessary to detect trends, *Mar. Pollut. Bull.*, doi:10.1016/j.marpolbul.2012.04.002, in press.

De'ath, G., and K. E. Fabricius (2010), Water quality as a regional driver of coral 1666 biodiversity and macroalgae on the Great Barrier Reef, *Ecol. Appl.*, *20*, 840–850.

Doney, S. C. (2010), The growing human footprint on coastal and open-ocean biogeochemistry, *Science*, *328*, 1512–1516.

Efron, B., and R. J. Tibshirani (1993), *An Introduction to the Bootstrap*, Chapman and Hall, New York.

Fritsch, F. N., and R. E. Carlson (1980), Monotone piecewise cubic interpolation, *SIAM J. Numer. Anal.*, *17*, 238–246.

Furnas, M. (2003), Catchment and corals: Terrestrial runoff to the Great Barrier Reef, report, Aust. Inst. of Mar. Sci., Townsville, Queensl., Australia.

Kalnay, E. (2003), *Atmospheric Modeling, Data Assimilation and Predictability*, Cambridge Univ. Press, New York.

Kohavi, R. (1995), A study of cross-validation and bootstrap for accuracy estimation and model selection, in *Proceedings of the Fourteenth International Joint Conference on Artificial Intelligence*, vol. 2, pp. 1137–1143, AAAI Press, Quebec, Quebec, Canada.

Kroon, F. J., P. M. Kuhnert, B. L. Henderson, S. N. Wilkinson, A. Kinsey-Henderson, B. Abbott, J. E. Brodie, and R. D. R. Turner (2012), River loads of suspended solids, nitrogen, phosphorus and herbicides delivered to the Great Barrier Reef lagoon, *Mar. Pollut. Bull.*, doi:10.1016/j.marpolbul.2011.10.018, in press.

Letcher, R. A., A. J. Jakeman, M. Calfas, S. Linforth, B. Baginska, and I. Lawrence (2002), A comparison of catchment water quality models and direct estimation techniques, *Environ. Modell. Software*, *17*, 77–85.

Lewis, S. E., G. Shields, B. Kamber, and J. Lough (2007), A multi-trace element coral record of land-use changes in the Burdekin River catchment, NE, Australia, *Palaeogeogr. Palaeoclimatol. Palaeoecol.*, *246*, 471–487.

Littlewood, I. G., and T. J. Marsh (2005), Annual freshwater river mass loads from Great Britain, 1975–1994: Estimation algorithm, database and monitoring network issues, *J. Hydrol.*, *304*, 221–237.

McCulloch, M., S. Fallon, T. Wyndham, E. Hendy, J. Lough, and D. Barnes (2003), Coral record of increased sediment flux to the inner Great Barrier Reef since European settlement, *Nature*, *421*, 727–730.

McIvor, J. G., J. Williams, and C. J. Gardener (1995), Pasture management influences runoff and soil movement in the semi-arid tropics, *Aust. J. Exp. Agric.*, *35*, 55–65.

McKergow, L. A., I. P. Prosser, A. O. Hughes, and J. E. Brodie (2005), Sources of sediment to the Great Barrier Reef World Heritage area, *Mar. Pollut. Bull.*, *51*, 200–211.

Mitchell, A. W., and M. J. Furnas (2001), River logger—A new tool to monitor riverine suspended particle fluxes, *Water Sci. Technol.*, *43*(9), 115–120.

Morehead, M. D., J. P. Syvitski, E. W. H. Hutton, and S. D. Peckham (2003), Modeling the temporal variability in the flux of sediment from ungauged river basins, *Global Planet. Change*, *39*, 95–110.

Nistor, C. J., and M. Church (2005), Suspended sediment transport regime in a debris-flow gully on Vancouver Island, British Columbia, *Hydrol. Processes*, *19*, 861–885.

Pagendam, D. E., and A. H. Welsh (2011), Statistical estimation of total discharge volumes, paper presented at MODSIM2011, 19th International Congress on Modelling and Simulation, Modell. and Simul. Soc. of Aust. and N. Z., Brisbane, Queensl., Australia.

Petheram, C., T. A. McMahon, and M. C. Peel (2008), Flow characteristics of rivers in northern Australia: Implications for development, *J. Hydrol.*, *357*, 93–111.

Pinheiro, J. C., and D. M. Bates (2000), *Mixed-Effects Models in S and S-Plus*, Springer, New York.

R Development Core Team (2005), *R: A Language and Environment for Statistical Computing, Reference Index Version 2.12.1*, R Found. for Stat. Comput., Vienna.

Reef Water Quality Protection Plan Secretariat (2009), Reef water quality protection plan 2009: For the Great Barrier Reef world heritage area and adjacent catchments, report, Queensl. Dep. of Premier and Cabinet, Brisbane, Queensl., Australia.

Rustomji, P., and S. Wilkinson (2008), Applying bootstrap resampling to quantify uncertainty in fluvial suspended sediment loads estimated using rating curves, *Water Resour. Res.*, *44*, W09435, doi:10.1029/2007WR 006088.

Scanlan, J. C., A. J. Pressland, and D. J. Myles (1996), Runoff and soil movement on mid-slopes in north-east Queensland grazed woodlands, *Rangeland J.*, *18*, 33–46.

Scarth, P., M. Byrne, T. Danaher, B. Henry, R. Hasset, J. Carter, and P. Timmers (2006), State of the paddock: Monitoring condition and trend in groundcover across Queensland, paper presented at 13th Australasian Remote Sensing Conference, BAE Syst., Canberra, ACT, Australia.

Schmidt, M., D. Tindall, K. Speller, P. Scarth, and C. Dougall (2010), *Ground cover management practices in cropping and improved pasture grazing systems: Ground cover monitoring using remote sensing, final report*, Dep. of Environ. and Resour. Manage., Queensland, Australia.

Thomas, R. B. (1985), Estimating total suspended sediment yield with probability sampling, *Water Resour. Res.*, *21*, 1381–1388.

Thomas, R. B. (1988), Monitoring baseline suspended sediment in forested basins: The effects of sampling of suspended sediment rating curves, *Hydrol. Sci. J.*, *33*, 499–514.

Thomas, R. B., and J. Lewis (1995), An evaluation of flow-stratified sampling for estimating suspended sediment loads, *J. Hydrol.*, *170*, 27–45.

Venables, W. N., and B. D. Ripley (1998), *Modern Applied Statistics With S-Plus*, 2nd ed., Springer, New York.

Walling, D. E. (1977), Assessing the accuracy of suspended sediment rating curves for a small basin, *Water Resour. Res.*, *13*, 531–538.

Wang, Y.-G., P. M. Kuhnert, and B. Henderson (2011), Load estimation with uncertainties from opportunistic sampling data—A semiparametric approach, *J. Hydrol.*, *396*, 148–157.

Wikle, C. K., and L. M. Berliner (2007), A Bayesian tutorial for data assimilation, *Physica D*, *230*, 1–16.

Wilkinson, S., I. P. Prosser, P. Rustomji, and A. Read (2009), Modelling and testing spatially distributed sediment budgets to relate erosion processes to sediment yields, *Environ. Modell. Software*, *24*, 489–501.

Wood, S. N. (2006), *Generalized Additive Models: An Introduction With R*, Chapman and Hall, Boca Raton, Fla.

Z. T. Bainbridge, J. E. Brodie, and S. E. Lewis, Centre for Tropical Water & Aquatic Ecosystem Research (TropWATER), Australian Tropical Sciences Innovation Precinct (ATSIP), Bldg. DB145, James Cook University, Townsville, QLD 4811, Australia.

B. L. Henderson, CSIRO Mathematics, Informatics and Statistics, GPO Box 664, Canberra, ACT 2601, Australia.

P. M. Kuhnert, CSIRO Mathematics, Informatics and Statistics, Private Bag 2, Glen Osmond, SA 5064, Australia. (petra.kuhnert@csiro.au)

S. N. Wilkinson, CSIRO Land and Water, GPO Box 1666, Canberra, ACT 2601, Australia.